Modeling of Spatially Dispersive Quadrupolar Metasurfaces

Karim Achouri[1], **Ville Tiukuvaara**[1] **and Olivier J. F. Martin**[1]

[1]Nanophotonics and Metrology Laboratory, Department of Microengineering,
École Polytechnique Fédérale de Lausanne, Route Cantonale, 1015 Lausanne, Switzerland
*corresponding author, E-mail: karim.achouri@a3.epfl.ch

Abstract

Metasurfaces are typically modeled using boundary conditions restricted to dipolar responses. While generally effective, this modeling approach suffers in the case of large incidence angles. To provide a better modeling accuracy, we derive a model that includes dipolar and quadrupolar responses as well as higher-order spatially dispersive effects. The effectiveness of this extended model is demonstrated by predicting the angular scattering of a dielectric metasurface up to grazing angles. This work is expected to be useful for designing spatial analog optical signal processing metasurfaces for incident beams with large angular spectra.

1. Introduction

In recent years, there has been a growing interest in the implementation of spatial optical analog processing metasurfaces [1–7]. To help designing such structures, one may employ conventional metasurface synthesis techniques, such as [8,9], which only include dipolar responses. As shown in [10], such dipolar models work well within the paraxial limit but start exhibiting significant errors for small wavelength-to-period ratios and/or large incidence angles. To overcome this limitation, we have extended the model to include multipolar responses and spatially dispersive interactions [11, 12].

2. Metasurface Modeling

A common approach to model a metasurface is to replace it by a fictitious zero-thickness sheet, supporting electric and magnetic dipolar polarizations, for which convenient boundary conditions may be formulated [8, 9, 13]. To improve the angular scattering modeling accuracy of such a dipolar model, we have extended it to include quadrupolar responses. The new boundary conditions, for a metasurface lying in the xy plane, are given by [10]

$$\begin{aligned}\hat{\mathbf{z}}\times\Delta\mathbf{E} = &-j\omega\mu\mathbf{M}_{\parallel}+\frac{k^2}{2\epsilon}\hat{\mathbf{z}}\times\left(\overline{\overline{Q}}\cdot\hat{\mathbf{z}}\right)\\ &-\frac{1}{\epsilon}\hat{\mathbf{z}}\times\nabla\left[P_z-\frac{1}{2}(\nabla_{\parallel}\hat{\mathbf{z}}+\hat{\mathbf{z}}\nabla_{\parallel}):\overline{\overline{Q}}\right] \quad (1a)\\ &+\frac{j\omega\mu}{2}\left(\overline{\overline{S}}-S_{zz}\overline{\overline{I}}\right)\cdot\nabla_{\parallel},\end{aligned}$$

$$\begin{aligned}\hat{\mathbf{z}}\times\Delta\mathbf{H} = &\,j\omega\mathbf{P}_{\parallel}+\frac{k^2}{2}\hat{\mathbf{z}}\times\left(\overline{\overline{S}}\cdot\hat{\mathbf{z}}\right)\\ &-\hat{\mathbf{z}}\times\nabla\left[M_z-\frac{1}{2}(\nabla_{\parallel}\hat{\mathbf{z}}+\hat{\mathbf{z}}\nabla_{\parallel}):\overline{\overline{S}}\right] \quad (1b)\\ &-\frac{j\omega}{2}\left(\overline{\overline{Q}}-Q_{zz}\overline{\overline{I}}\right)\cdot\nabla_{\parallel}.\end{aligned}$$

where $\Delta\mathbf{E}$ and $\Delta\mathbf{H}$ are the differences of the fields on both sides of the metasurface, $\mathbf{P}$ and $\mathbf{M}$ are electric and magnetic dipolar responses, and $\overline{\overline{Q}}$ and $\overline{\overline{S}}$ are electric and magnetic quadrupolar responses. These multipolar quantities represent the response of the metasurface to an arbitrary excitation and include spatially dispersive interactions. They are related to the average fields and fields derivatives at the metasurface via

$$\begin{bmatrix}P_i\\M_i\\Q_{il}\\S_{il}\end{bmatrix}=\overline{\overline{\chi}}\cdot\begin{bmatrix}E_{\text{av},j}\\H_{\text{av},j}\\\nabla_k E_{\text{av},j}\\\nabla_k H_{\text{av},j}\end{bmatrix}, \quad (2)$$

where the hypersusceptibility tensor $\overline{\overline{\chi}}$ is given by

$$\overline{\overline{\chi}}=\begin{bmatrix}\epsilon_0\chi_{\text{ee}}^{ij} & \frac{1}{c_0}\chi_{\text{em}}^{ij} & \frac{\epsilon_0}{2k_0}\chi_{\text{ee}}^{'ijk} & \frac{1}{2c_0k_0}\chi_{\text{em}}^{'ijk}\\ \frac{1}{\eta_0}\chi_{\text{me}}^{ij} & \chi_{\text{mm}}^{ij} & \frac{1}{2\eta_0k_0}\chi_{\text{me}}^{'ijk} & \frac{1}{2k_0}\chi_{\text{mm}}^{'ijk}\\ \frac{\epsilon_0}{k_0}Q_{\text{ee}}^{ilj} & \frac{1}{c_0k_0}Q_{\text{em}}^{ilj} & \frac{\epsilon_0}{2k_0^2}Q_{\text{ee}}^{'iljk} & \frac{1}{2c_0k_0^2}Q_{\text{em}}^{'iljk}\\ \frac{1}{\eta_0k_0}S_{\text{me}}^{ilj} & \frac{1}{k_0}S_{\text{mm}}^{ilj} & \frac{1}{2\eta_0k_0^2}S_{\text{me}}^{'iljk} & \frac{1}{2k_0^2}S_{\text{mm}}^{'iljk}\end{bmatrix}. \quad (3)$$

These equations show that a quadrupolar metasurface provides a large number of additional degrees of freedom compared to a dipolar one. However, note that several important properties related to the symmetries of quadrupolar tensors, reciprocity and passivity/losslessness reduce the number of independent parameters in (3), as explained in [14].

In order to demonstrate the performance of our model, we compare its angular scattering predictive accuracy to that of the conventional dipolar model. Consider the simulation setup presented in Fig. 1a, where a metasurface made of dielectric cylinders is illuminated at oblique incidence by a TM-polarized wave. Its transmission coefficient is plotted versus wavelength and incidence angle in Fig. 1b. The performance of the dipolar model is first investigated by setting $\overline{\overline{Q}}=\overline{\overline{S}}=0$ in (1), substituting the fields by those obtained from full-wave simulation at $\theta=0^\circ$ and solving for the remaining non-zero susceptibilities. The latter

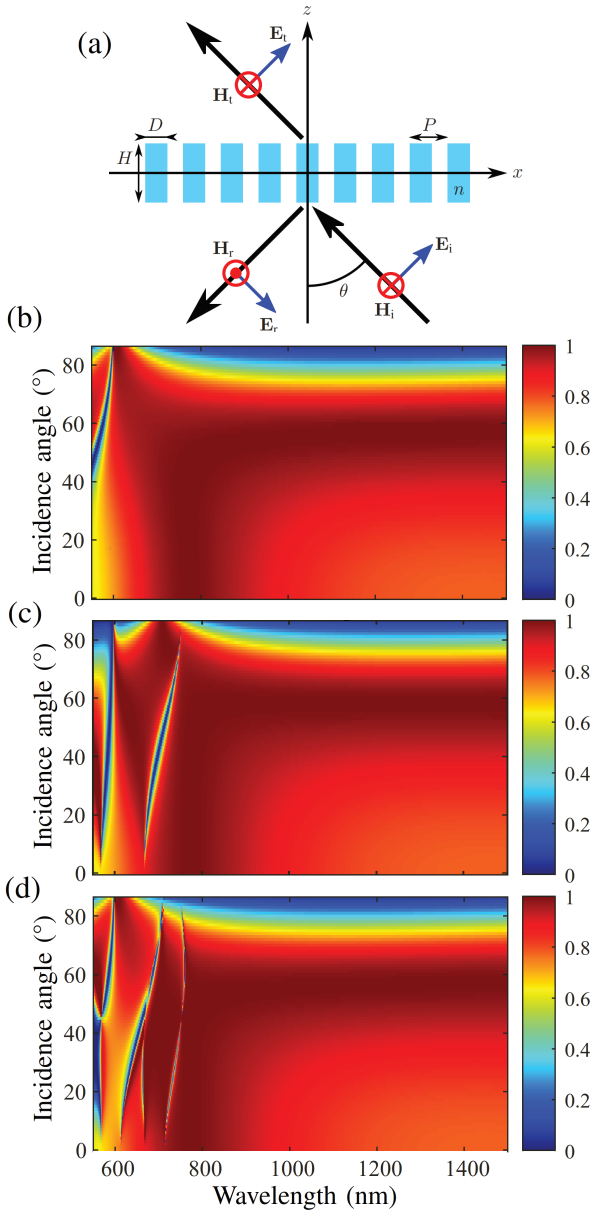

Figure 1: Multipolar modeling of an array of dielectric cylinders with $P = 225$ nm, $D = 200$ nm, $H = 200$ nm and $n = 2.55$. (a) Simulation setup. (b) Full-wave simulated transmission amplitude. Predicted transmission amplitude using a (c) purely dipolar and a (d) quadrupolar metasurface model. See [10] for more information.

are then used to predict the transmission coefficient in the range $\theta =]0°, 85°]$ and the resulting prediction is plotted in Fig. 1c. As expected, the model performs well for large wavelengths and small incidence angles but significant errors appear at lower wavelengths and higher angles. Now, the same approach is used for the quadrupolar model. Since more hypersusceptibility components must be solved, the full-wave simulated fields at $\theta = 0°, 45°$ and $85°$ are used to predict the transmission for all other angles. The result is plotted in Fig. 1d and, besides some undesired sharp features, show a much better agreement with the expected response, which is about 3.5 better than the dipolar model in Fig. 1c.

Acknowledgement

We gratefully acknowledge funding from the Swiss National Science Foundation (project PZ00P2_193221).

References

[1] A. Pors, M. G. Nielsen, and S. I. Bozhevolnyi, "Analog Computing Using Reflective Plasmonic Metasurfaces," *Nano Lett.*, vol. 15, no. 1, pp. 791–797, 2015.

[2] A. Chizari, S. Abdollahramezani, M. V. Jamali, and J. A. Salehi, "Analog optical computing based on a dielectric meta-reflect array," *Opt. Lett.*, vol. 41, no. 15, p. 3451, 2016.

[3] S. Abdollahramezani, A. Chizari, A. E. Dorche, M. V. Jamali, and J. A. Salehi, "Dielectric metasurfaces solve differential and integro-differential equations," *Opt. Lett.*, vol. 42, no. 7, p. 1197, 2017.

[4] H. Babashah, Z. Kavehvash, S. Koohi, and A. Khavasi, "Integration in analog optical computing using metasurfaces revisited: Toward ideal optical integration," *J. Opt. Soc. Am. B*, vol. 34, no. 6, p. 1270, 2017.

[5] T. Zhu, Y. Zhou, Y. Lou, H. Ye, M. Qiu, Z. Ruan, and S. Fan, "Plasmonic computing of spatial differentiation," *Nat. Commun.*, vol. 8, no. 1, p. 15391, 2017.

[6] A. Momeni, H. Rajabalipanah, A. Abdolali, and K. Achouri, "Generalized Optical Signal Processing Based on Multioperator Metasurfaces Synthesized by Susceptibility Tensors," *Phys. Rev. Applied*, vol. 11, no. 6, p. 064042, 2019.

[7] X. Zhang, Q. Li, F. Liu, M. Qiu, S. Sun, Q. He, and L. Zhou, "Controlling angular dispersions in optical metasurfaces," *Light Sci. Appl.*, vol. 9, no. 1, p. 76, 2020.

[8] C. L. Holloway, E. F. Kuester, J. A. Gordon, J. O'Hara, J. Booth, and D. R. Smith, "An Overview of the Theory and Applications of Metasurfaces: The Two-Dimensional Equivalents of Metamaterials," vol. 54, no. 2, pp. 10–35, 2012.

[9] C. Caloz and K. Achouri, *Electromagnetic Metasurfaces: Theory and Applications*. Hoboken, NJ: Wiley-IEEE Press, 2021.

[10] K. Achouri, V. Tiukuvaara, and O. J. F. Martin, "Multipolar modeling of spatially dispersive metasurfaces," *arXiv preprint arXiv:2103.10345*, 2021.

[11] R. E. Raab and O. L. De Lange, *Multipole Theory in Electromagnetism: Classical, Quantum, and Symmetry Aspects, with Applications*. No. 128 in Oxford Science Publications, Oxford University Press, 2005.

[12] C. Simovski, *Composite media with weak spatial dispersion*. Singapore: Pan Stanford, 2018.

[13] M. Idemen, *Discontinuities in the electromagnetic field*. Piscataway, NJ Hoboken, New Jersey: IEEE Press Wiley, 2011.

[14] K. Achouri and O. J. F. Martin, "Extension of lorentz reciprocity and poynting theorems for spatially dispersive media with quadrupolar responses," *Phys. Rev. B*, vol. 104, p. 165426, 2021.